I.I. Sanduleac

I.I. Sanduleac

Technical University of Moldova
168, Stefan cel Mare Ave.,
Chisinau, MD-2004, Moldova

THERMOELECTRIC POWER FACTOR OF TTT_2I_3 QUASI-ONE-DIMENSIONAL CRYSTALS IN THE 3D PHYSICAL MODEL

Tetrathiotetracene – Iodide organic crystals (TTT_2I_3) are very promising materials for thermoelectric applications. Due to their pronounced quasi-one-dimensionality, the density of states is increased in the direction of molecular chains and, respectively, the Seebeck coefficient is also increased. In addition, partial compensation of two main electron-phonon interactions leads to significant increase of carriers' mobility, ensuring high values of electrical conductivity. However, the mobility is diminished by the scattering on impurities and by the interchain interaction. Theoretically, it was predicted a power factor values up to 0.03 W/m·K^2 for crystals with increased purity. Initially, the estimations were performed in the frame of a simplified one-dimensional (1D) model, neglecting the weak interchain interaction. Further investigations have shown that for ultra-pure crystals this interaction becomes important and the calculations should be performed in the frame of a more realistic 3D model. In this paper, the electrical conductivity, Seebeck coefficient and the power factor for TTT_2I_3 organic crystals are presented in a 3D model. Also, the criteria of applicability of the simplified 1D model are estimated.

Key words: thermoelectricity, tetrathiotetracene iodide, interchain interaction, three-dimensional crystal model.

Introduction

In recent years, increasing attention has been paid to a search for new nanostructured thermoelectric materials, especially of organic type, with improved figure of merit *ZT*. The design and development of high-efficient thermoelectric devices which will be able to provide widespread conversion of low level heat into electricity and vice versa, represent a promising challenge for scientists. A big figure of merit requires that the given material have low thermal conductivity, increased electrical conductivity and high Seebeck coefficient. Different compounds with complex crystalline structure, like clathrates and skutterudites were reported to have very good thermoelectric figure of merit: $ZT \sim 1 \div 1.5$ at $T = 800 \div 1000$ K [1 - 3]. In these materials, the atoms are loosely bonded and the phonon scattering is increased, which leads to the diminution of thermal conductivity. In the same time, the electrical conductivity practically does not change. The Zintl compounds with large elementary cell, $Yb_{14}MnSb_{11}$, $Yb_{11}GaSb_9$, $Ca_{11}GaSb_9$ and $SrZnSb_2$, were reported to have low thermal conductivity due to the high fraction of low-velocity acoustical phonon modes [4].

High density of electronic states (DOS) may be achieved in low-dimensional systems, like superlattices, nanowires and quantum dots: while the system size decreases, the electronic DOS splits and becomes narrow [5]. This fact leads to very good thermoelectric properties: in Bi_2Te_3/Sb_2Te_3 superlattices $ZT \sim 2.5$ and in superlattices with quantum dots *PbTe*/*PbSe*, $ZT \sim 3$ at 600 K have measured [6, 7].

Nanostructured organic materials have the priority to join together the properties of low-dimensional system and those of multi-component material with much more diverse and complicated interactions. Also, their diverse properties are well tunable through molecular chemistry and doping procedures. Very interesting investigations are provided in last years, revealing promising results: in poly (3, 4-ethylenedioxythiophene) (PEDOT), a maximum $ZT = 0.42$ has been achieved by minimizing the total dopant volume [8]. The 2,7-Dialkyl [1] benzothieno [3,2-b] [1] benzothiophene derivatives have shown huge carrier mobility [10]. The implementation of organic nanostructured materials in the industry of thermoelectric devices has very good prospects, so as the production technology is not expensive and these materials are friendly with environment [9]. Theoretical investigations of thermoelectric properties of quasi-one-dimensional organic crystals of TTT_2I_3 [11, 16, 18] have demonstrated that the latter may be promising candidates for thermoelectric applications.

The aim of this paper is to model the electrical conductivity, Seebeck coefficient and the power factor of TTT_2I_3 organic crystals in the frame of a more complete 3D physical model and to determine the criteria, when the simpler 1D model may be used. Also, the possibilities to increase the thermoelectric figure of merit are analyzed.

Three-dimensional crystal model for TTT_2I_3 organic crystals

The basic structure of TTT_2I_3 organic crystal is primarily determined by the *TTT* molecules. The orthorhombic crystal structure consists of segregate donor *TTT* and acceptor iodine stacks. The interplanar distance of *TTT* molecules in stacks is identical and equals 3.32 Å, ensuring significant overlap of π-wave functions along stacks and an electrical conductivity of band type in this direction. The sulfur-sulfur distance on adjacent *TTT* molecules is 3.73 Å. This short sulfur contact provides a small interchain interaction which will be taken into account in this paper. The overlap of wave functions in transversal direction is small and the electrical conductivity is of hopping type. Parallel to the longitudinal ***b*** direction the iodine atoms lie in 4 columns per unit cell projection area [12, 13]. The elementary cell is very near to a parallelepiped. A Cartesian coordinate system is considered with the *x*-axis lying in the ***b*** direction and *y*, *z* – in the ***a*** and ***c*** directions, respectively.

The charge transport is of *p*-type: two *TTT* molecules give one electron to iodine chain. The last one has very low electrical conductivity. In the *x* direction, the overlap of HOMO of *TTT* molecules generates a narrow conduction band (~ 25 k_0T_0, T_0 is the room temperature; the transfer energy in *x*-direction is 0.16 eV). In the transversal directions there are two *TTT* molecules per lattice constant (*a* and *c*). The transfer energies in the *y* and *z* directions, w_2 and w_3, are estimated on the base of experimental measurements of the electrical conductivity in the transversal and longitudinal directions. Two parameters are introduced, d_1 and d_2, as it follows: $d_1 = w_2/w_1 = \sigma_{yy}/\sigma_{xx}$ and $d_2 = w_3/w_1 = \sigma_{zz}/\sigma_{xx}$. The internal structure of TTT_2I_3 crystals is strong quasi-one-dimensional ($d_1 \approx d_2 = 0.013$). Due to the property to allow non-stoichiometric compounds, the optimization of iodine content which determines the holes concentration, will generate more efficient TTT_2I_3 – based devices with improved thermoelectric figure of merit, *ZT* [12, 14].

The Hamiltonian of the system was described earlier [15, 16] for the 2D case. Now it has the form:

$$H = \sum_{\boldsymbol{k}} E(\boldsymbol{k}) a_{\boldsymbol{k}}^{+} a_{\boldsymbol{k}} + \sum_{\boldsymbol{q}} \hbar\omega_{\boldsymbol{q}} b_{\boldsymbol{q}}^{+} b_{\boldsymbol{q}} + \sum_{\boldsymbol{k},\boldsymbol{q}} A(\boldsymbol{k},\boldsymbol{q}) a_{\boldsymbol{k}}^{+} a_{\boldsymbol{k}+\boldsymbol{q}} (b_{\boldsymbol{q}} + b_{-\boldsymbol{q}}^{+}) + \sum_{n,j} I V_0 a_j^{+} a_j \delta(\boldsymbol{r}_n - \boldsymbol{r}_j). \quad (1)$$

Here the first term is for carriers (holes) in the tight binding and nearest neighbors' approximations. The energy of carrier measured from the extremum of the band has the form:

$$E(\boldsymbol{k}) = -2w_1\cos(k_x b) - 2w_2\cos(k_y a) - 2w_3\cos(k_z c), \tag{2}$$

where k_x, k_y, k_z are the projections of the quasi-wave vector $\boldsymbol{k}$.

The second term in (1) is the energy of longitudinal acoustic phonons:

$$\omega_{\boldsymbol{q}}^2 = \omega_1^2\sin^2(q_x b/2) + \omega_2^2\sin^2(q_y a/2) + \omega_3^2\sin^2(q_z c/2), \tag{3}$$

where ω_1, ω_2 and ω_3 are limit frequencies in the *x, y* and *z* directions, (q_x, q_y, q_z) are the projections of the quasi-wave vector $\boldsymbol{q}$, $\omega_2 \approx \omega_3 << \omega_1$.

As it was mentioned in [17], the cross transversal vibrations have negligible small effect and the simple 1D phononic spectrum is sufficient enough to describe thermoelectric properties.

The third term in (1) describes the electron-phonon interaction. It contains two main mechanisms. The first is determined by the variation of transfer integrals with respect to the intermolecular distances (the mechanism of the deformation potential). The second mechanism is similar to that of polaron: the lattice vibrations lead to the variation of the polarization energy of molecules surrounding the charge carrier.

The square module of the matrix element of electron-phonon interaction has the form:

$$\begin{aligned}|A(\boldsymbol{k},\boldsymbol{q})|^2 = 2\hbar/(NM\omega_{\boldsymbol{q}})\{w_1'^2[\sin(k_x b) - \sin(k_x - q_x, b) + \gamma_1\sin(q_x b)]^2 + \\ w_2'^2[\sin(k_y a) - \sin(k_y - q_y, a) + \gamma_2\sin(q_y a)]^2\} + w_3'^2[\sin(k_z c) - \sin(k_z - q_z, c) + \gamma_3\sin(q_z c)]^2\}.\end{aligned} \tag{4}$$

Here γ_1, γ_2 and γ_3 are the parameters describing the ratio of amplitudes of polaron-type interaction to the deformation potential one in the *x*, *y* and *z* directions [15], w_1', w_2' and w_3' are the derivatives of transfer energies with respect to intermolecular distance.

The last term in (1) describes the scattering of charge carriers on impurity centers, which are considered point-like, electric neutral and randomly distributed; *I* is the energy of interaction of a hole with the impurity center, V_0 is the volume of interaction region. The summation is provided on all the impurity centers in the base region of the crystal.

Transport phenomena

The scattering probability takes the form [15]:

$$W(\boldsymbol{k},\boldsymbol{k}') = 2\pi k_0 T/(\hbar^2\omega_q|A(\boldsymbol{k}+\boldsymbol{q},\boldsymbol{q})|^2)\delta[\varepsilon(k_x+q_x) - \varepsilon(k_x)], \tag{5}$$

where delta-function contains two main approximations – the scattering processes on phonons are considered elastic at room temperature and the energies w_2 and w_3 are neglected in comparison with w_1. The linearized kinetic equation is solved analytically and the expression for electrical conductivity takes the form:

$$\sigma_{xx}(0) = -\frac{8e^2w_1^2a^2}{k_0TV\hbar^2}\sum_{\boldsymbol{k}}\sin^2(k_x b)n_{\boldsymbol{k}}(1-n_{\boldsymbol{k}})/\sum_{\boldsymbol{k}'}W(\boldsymbol{k},\boldsymbol{k}')[1 - v_x(k_x')/v_x(k_x)], \tag{6}$$

where $v_x(k)$ is the projection of carrier velocity on *x* direction. The quasi-wave vector $\boldsymbol{k}$ has quasi-continuous spectrum and the summation may be replaced by integration over the entire Brillouin zone. In this order, the transport integrals are defined as:

$$R_n = abc\int_0^{\pi/a}dk_x\int_0^{\pi/b}dk_y\int_0^{\pi/c}dk_z\sin^3(k_x b)n_{\boldsymbol{k}}(1-n_{\boldsymbol{k}})\times \tag{7}$$

$$\frac{[\varepsilon - (1+d_1+d_2)\varepsilon_F]^n}{(1-\gamma_1\cos(k_x b))^2 + \frac{1}{4\sin^2(k_x b)}\{d_1^2[1+\gamma_2^2+2\sin^2(k_y a) - 2\gamma_2\cos(k_y a)] + d_2^2[1+\gamma_3^2+2\sin^2(k_z c) - 2\gamma_3\cos(k_z c)]\} + D_0}.$$

Here $\varepsilon = E(\boldsymbol{k})/2w_1$, $\varepsilon_F = E_F/2w_1$ are the energy of carriers and the Fermi energy in the unities of $2w_1$, $n_{\boldsymbol{k}}$ is the Fermi distribution function for carriers with energy (2), D_0 is the parameter describing the scattering of carriers on impurity centers:

$$D_0 = n_{im}^{3D} I^2 V_0^2 \frac{Mv_s^2}{4b^3 acw_1'^2 k_0 T}, \tag{8}$$

where n_{im}^{3D} is the concentration of impurity.

The expression for electrical conductivity takes the form:

$$\sigma_{xx} = \sigma_0 R_0, \text{ where } \sigma_0 = \frac{2e^2 w_1^3 v_{s1}^2 Mr}{\pi^3 abc\hbar (k_0 T)^2 w_1'^2}, \tag{9}$$

here $r = 4$ is the number of molecular chains through the transversal section of the elementary cell, v_{s1} is the sound velocity along the chains, M is the mass of TTT molecule and w_1' is the derivative of transfer energy with respect to intermolecular distance.

The Seebeck coefficient and the power factor are defined as:

$$S_{xx} = (k_0 / e)(2w_1 / k_0 T) R_1 / R_0. \tag{10}$$

Results and discussions

Numerical calculations for crystals with different degrees of purity were made in the frame of the 3D and 1D models. The crystal parameters are: $M = 6.5 \cdot 10^5 m_e$ (m_e is the free electron mass), $a = 18.35$ Å, $b = 4.97$ Å, $c = 18.46$ Å, $v_{s1} = 1.5 \cdot 10^3$ m/s, $w_1 = 0.16$ eV, $w_1' = 0.26$ eVÅ^{-1} [18]. The mean polarizability of TTT molecules, $\alpha_0 = 46$ Å^{-3} and this leads to $\gamma_1 = 1.7$. The parameters γ_2 and γ_3 are calculated from the relations $\gamma_2 = \gamma_1 b^5 / (a^5 d)$ and $\gamma_3 = \gamma_1 b^5 / (c^5 d)$. The values of lattice constants a and c are very close so it is possible to approximate $\gamma_2 \approx \gamma_3$.

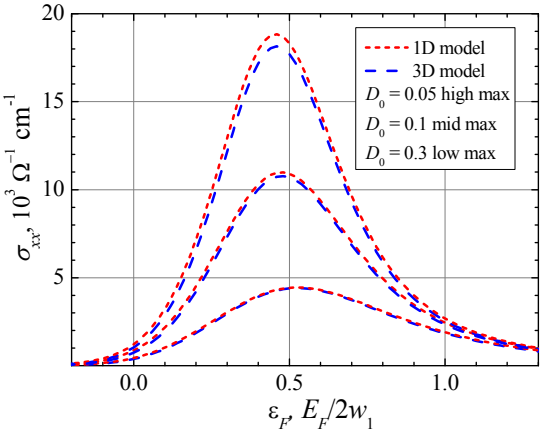

Fig. 1. Electrical conductivity as function of dimensionless Fermi energy for $D_0 = 0.3, 0.1, 0.05$.

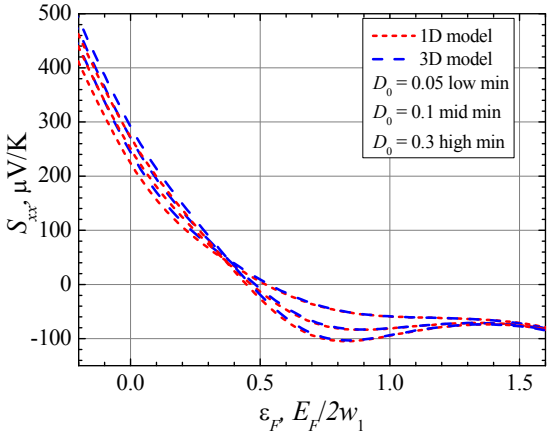

Fig.2. Thermopower S_{xx} as function of dimensionless Fermi energy.

In Fig. 1 the electrical conductivity in the x direction for p-type TTT_2I_3 crystals as function of dimensionless Fermi energy is presented for $D_0 = 0.3$, 0.1, 0.05. One can observe the pronounced quasi-one-dimensionality of the crystal: the influence of interchain interaction on the transport properties along the molecular chains is weak and becomes distinguishable only for high purity level. In the crystals synthesized from gaseous phase ($D_0 = 0.1$) it was reported $\sigma_{xx} \sim 10^4$ Ω^{-1}cm^{-1} [13]. The diminution of impurity center concentration, as it results from theory, leads to the increase of the

electrical conductivity and, consequently, of the power factor P_{xx}. Another way to improve P_{xx} is the optimization of the concentration of holes (by varying the concentration of iodine acceptors) due to the property of the crystal to allow non-stoichiometric compounds.

In Fig. 2 the Seebeck coefficient (S_{xx}) as function on dimensionless Fermi energy at room temperature is presented. For *p*-type crystals, S_{xx} takes positive values. It is observed the reverse situation-in order to increase P_{xx} it is needed to diminish the holes concentration, with respect to the stoichiometric one, since this procedure provides usually high Seebeck coefficient values. Seebeck coefficient is less sensitive to the interchain interaction. Experimentally it was reported $S = 36$ μV·K^{-1} for crystals with $\sigma = 1200$ Ω^{-1}cm^{-1} [12, 19].

In Fig. 3 the power factor (P_{xx}) as function of dimensionless Fermi energy is presented. The corrections induced by the realistic 3D model are ~10% when $D_0 = 0.05$ and $\varepsilon_F = 0.33$ (or stoichiometric concentration). For experimentally reported crystals with $D_0 = 0.1$ the deviations of the 3D model are smaller and the predictions made in the frame of 1D model are applicable. Recent researches in high conductive PEDOT: PSS/graphene composites have reported a power factor of 45.7 μW·m^{-1}·K^{-2} [20].

As it is observed, the interchain interaction becomes important when the crystal purity is increased.

In order to determine the criterion, when the 1D approximation is still possible, new numerical calculations were also made for another set of ultra-pure crystals with $D_0 = 0.04$, 0.03, 0.02 and higher electrical conductivities not obtained yet. In the purest crystal the predicted conductivity achieves quite large values, of the order 3.5×10^4 Ω^{-1}cm^{-1}, (Fig.4). For stoichiometric crystals $\sigma_{xx} = 16$; 20; and 26×10^3 Ω^{-1}cm^{-1} and the relative corrections induced by the new 3D model are: 6%, 7.3% and 9.5%, respectively.

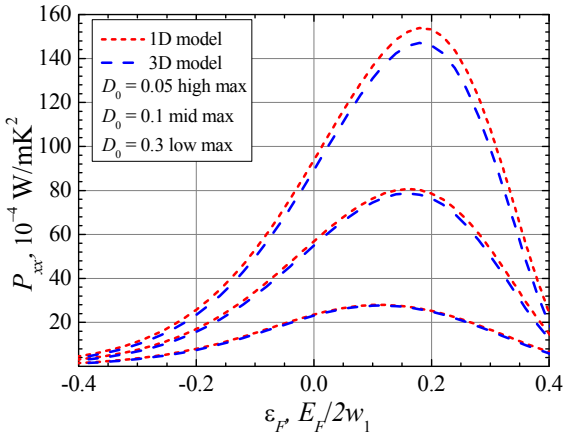

Fig.3. Power factor P_{xx} as function of dimensionless Fermi energy.

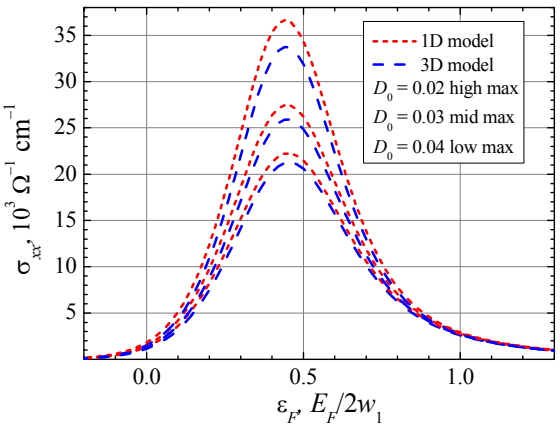

Fig. 4. Electrical conductivity σ_{xx} as function of dimensionless Fermi energy for purer crystals.

In Fig. 5 the Seebeck coefficient is presented as function of dimensionless Fermi energy (ε_F) for ultra-pure crystals. In this case, the differences between 3D and 1D model are more distinguishable, bud remains negligible.

The power factor is presented in Fig. 6. As well as the electrical conductivity, the power factor is sensible to the height of the relaxation time maximum, determined by partial compensation of above mentioned electron-phonon interactions. In the not very pure crystals with high impurity concentrations the relaxation time maximum and the carrier mobility is limited by scattering on impurities and the scattering on the nearest chains may be neglected.

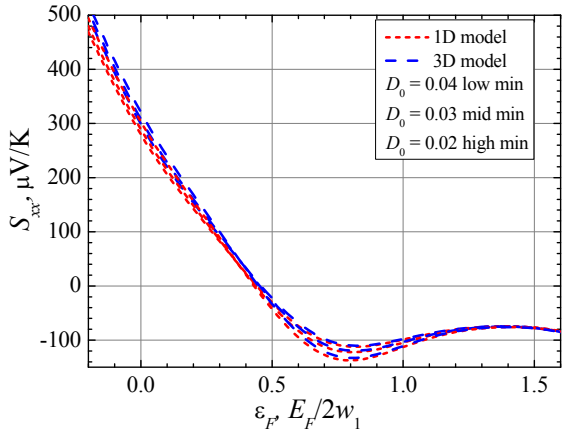

Fig.5. Seebeck coefficient as function of dimensionless Fermi energy for purer crystals.

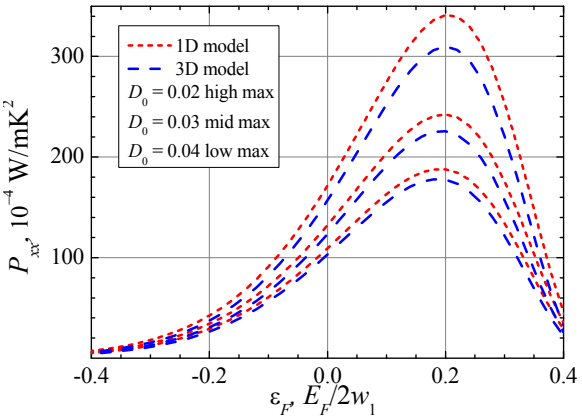

Fig.6. Power factor as function of dimensionless Fermi energy for purer crystals.

In this case the 1D model is a good approximation. In the purer crystals the scattering on the nearest chains begins to limit the height of relaxation time maximum and the mobility. The corrections for P_{xx} made by the new 3D model are: 11%, 13%, and 16%, for D_0 = 0.04, 0.03, 0.02 and stoichiometric crystals with $\varepsilon_F = 0.33$. Thus, for TTT_2I_3 crystals with electrical conductivity $\sigma_{xx} > 3\times10^4$ Ω^{-1}cm^{-1} it is necessary to apply the 3D physical model.

Conclusions

A more realistic 3D physical model for tetrathiotetracene-iodide organic crystals, TTT_2I_3 is developed by taking into account the interaction of nearest neighbors molecular chains. Two series of the parameter D_0 which describes the carrier scattering on impurities, are considered: for less pure and purer crystals. It is shown that the simplified 1D model is applicable for not very pure crystals, while for ultra-pure crystals with electrical conductivity $\sigma_{xx} > 3\times10^4$ Ω^{-1}cm^{-1}, the interchain interaction becomes significant and the 3D model it is needed to be used. When applying this new physical model for stoichiometric crystals, grown from vapor phase [13] with $D_0 = 0.1$, the predicted values for electrical conductivity, Seebeck coefficient and the power factor are: $\sigma_{xx} = 8.3\times10^4$ Ω^{-1}cm^{-1}, $S_{xx} = 68\times10^{-6}$ V/K, $P_{xx} = 39\times10^{-4}$ W/m·K^2. Maximum value of P_{xx} in this case achieves 80×10^{-4} W/m·K^2 or two times higher than in Bi_2Te_3, the widest used commercial material, very good result.

Acknowledgements

The author expresses gratitude to A. Casian for valuable guidance and advices, and acknowledges the financial support of EU Commission FP7 program under the grant no. 308768.

References

1. B. C. Sales, D. Mandrus, R.K. Williams, Filled Skutterudite Antimonides: A New Class of Thermoelectric Materials, *Science* **272**, 1325-1328, 1996.
2. G. S. Nolas, D. T. Morelli, T. M. Tritt, A Phonon-Glass-Electron Crystal Approach to Advanced Thermoelectric Energy Conversion Applications, *Annu. Rev. Mater. Sci.* **29**, 89, 1999.
3. G. S. Nolas, J. L. Cohn, G. A. Slack, S. B. Schujman, Semiconducting Ge clathrates: Promising candidates for thermoelectric applications, *Appl. Phys. Lett.* **73**, 178, 1998.

4. E. S. Toberer, A. F. May, G. J. Snyder, Zintl Chemistry for Designing High Efficiency Thermoelectric Materials, *Chem. Mater.* **22**, 624, 2010.
5. L. D. Hicks, M. S. Dresselhaus, Effect of quantum-well structures on the thermoelectric figure of merit, *Phys. Rev.* **47**, 12727, 1993.
6. R. Venkatasubramanian, E. Siivola, T. Colpitts, B. O'Quinn, Thin-film thermoelectric devices with high room-temperature figures of merit, *Nature* **413**, 597, 2001.
7. T. C. Harman, P. J. Taylor, M. P. Walsh, B. E. LaForge, Quantum Dot Superlattice Thermoelectric Materials and Devices, *Science* **297**, 2229, 2002.
8. G. Kim, L. Shao, K. Zhang, K. P. Pipe, Engineered doping of organic semiconductors for enhanced thermoelectric efficiency, Nat. Mater. **12**, 719, 2013.
9. Q. Zhang, Y. Sun, W. Xu and D. Zhu, Organic Thermoelectric Materials: Emerging Green Energy Materials Converting Heat to Electricity Directly and Efficiently, *Adv. Materials*, **31**, 2014.
10. W. Shi, J. Chen, J. Xi, D. Wang, and Z. Shuai, Search for Organic Thermoelectric Materials with High Mobility: The Case of 2,7-Dialkyl[1]benzothieno[3,2-b][1]benzothiophene Derivatives, *Chem. Mater*. **26**, 2669, 2014.
11. A. I. Casian, I. I. Sanduleac, Organic Thermoelectric Materials: new opportunities, *J. of Thermoelectricity*, **3**, 2013.
12. L. Isett, Magnetic susceptibility, electrical resistivity, and thermoelectric power measurements of *bis*(tetrathiotetracene)-triiodide, *Phys.Rev*. **B18**, 1978.
13. B. Hilti, C. Mayer, Electrical Properties of the Organic Metallic Compound bis (Tetrathiotetracene)-Triiodide, $(TTT)_2I_3$, *Helvetica Chimica Acta*, **61**(40), 501, 1978.
14. G. Kim, L. Shao, K. Zhang, K. P. Pipe, Engineered doping of organic semiconductors for enhanced thermoelectric efficiency, *Nat. Mater*. **12**, 719, 2013.
15. A. I. Casian, I. I. Sanduleac, Effect of Interchain Interaction on Electrical Conductivity in Quasi-One-Dimensional Organic Crystals of Tetrathiotetracene-Iodide, *J. of Nanoelectronics and Optoelectronics*, **7**, 706-711, 2012.
16. I. I. Sanduleac, A. I. Casian, J. Pflaum, Thermoelectric Properties of Nanostructured Tetrathiotetracene Iodide Crystals in a Two-Dimensional Model, *Journal of Nanoelectronics and Optoelectronics,* **9**, 247-252, 2014.
17. I. I. Sanduleac, Effect of 2D phonon spectrum on the electrical conductivity and thermopower of tetrathiotetracene-iodide crystals, *MJPS*, in press, 2014.
18. A. I. Casian, J. G. Stockholm, V. Dusciac and V. Nicic, Low-Dimensional Organic Crystal Tetrathiotetracene–Iodide as Thermoelectric Material: Reality and Prospects, *J. Nanoelectronics and Optoelectronics*, **4**, 95, 2009.
19. P.M. Chaikin, G. Gruner, I.F. Shchegolev and E.B. Yagubskii, Thermoelectric power of $TTT_2I_{3+\delta}$, *Solid State Communications*, **32**, 1211, 1979.
20. D. Yoo, J. Kim, J. H. Kim, Direct synthesis of highly conductive poly(3,4-ethylenedioxythiophene):poly(4-styrenesulfonate) (PEDOT:PSS)/grapheme composites and their applications in energy harvesting systems, *Nano Research*, **7**, Issue 5, 717-730, 2014.

Submitted 29.08.14